# Technical Note

1971-2

## An Analysis of Finite Rise and Fall Time Current Excitation of TRAPATT Diodes

T. G. Bryant
J. D. Welch

7 January 1971

Prepared under Electronic Systems Division Contract F19628-70-C-0230 by

**Lincoln Laboratory**

MASSACHUSETTS INSTITUTE OF TECHNOLOGY

Lexington, Massachusetts

MASSACHUSETTS INSTITUTE OF TECHNOLOGY

LINCOLN LABORATORY

# AN ANALYSIS OF FINITE RISE AND FALL TIME CURRENT EXCITATION OF TRAPATT DIODES

*T. G. BRYANT*

*Group 36*

*J. D. WELCH*

*Group 41*

TECHNICAL NOTE 1971-2

7 JANUARY 1971



LEXINGTON MASSACHUSETTS

The work reported in this document was performed at Lincoln Laboratory, a center for research operated by Massachusetts Institute of Technology, with the support of the Department of the Air Force under Contract F19628-70-C-0230.

## ABSTRACT

Several recent papers have treated the high efficiency avalanche diode using a simplified analysis which successfully explains the principal features of the traveling avalanche zone, formation of the trapped plasma, and plasma extraction. These analyses have assumed square wave current excitation so that all phenomena occur under constant current conditions. In this paper it is shown that the square wave current excitation requires negative impedance terminations above the 5th harmonic. Since the harmonic amplitudes in a square wave decrease only as 1/n, harmonics as high as the 9th and 11th must be properly terminated to make the analysis realistic and to prevent premature avalanche. We have analyzed the TRAPATT operation using the same physical approximations for plasma formation and recovery as used in the previous square wave analyses. However, we have assumed a trapezoidal current waveform which contains primarily first and third harmonics with negligibly small higher harmonics. In this analysis the avalanche zone transit and portions of the plasma extraction process occur while the current is changing. The resulting device voltage is calculated as a continuous analytical function of time except during the plasma formation interval and the final saturated velocity phase of the plasma extraction interval, where an interpolated voltage waveform is obtained. Fourier analysis of the voltage waveform provides the device efficiency as well as the necessary circuit termination at the 1st and 3rd harmonics. Realizability conditions on the diode parameters are also obtained.



Accepted for the Air Force
Joseph R. Waterman, Lt. Col., USAF
Chief, Lincoln Laboratory Project Office

# AN ANALYSIS OF FINITE RISE AND FALL TIME CURRENT EXCITATION OF TRAPATT DIODES

## I. Introduction

An analysis is presented for the operation of an avalanche diode oscillator in the "trapped plasma" mode when excited by a finite rise-time (trapezoidal) current waveform. Previous papers[1,2,3] analyzing the operation of the trapped plasma mode have detailed the traveling ionization zone, formation of the trapped plasma, and the exit of the plasma under constant current driving conditions. Furthermore, in Refs. 1 and 2 approximate closed form analytical solutions have been presented for calculating a complete cycle of the steady state voltage waveform assuming an ideal square wave current drive. The analysis using a square wave current provides considerable insight into the details of the trapped plasma cycle. This paper extends the analysis to handle a somewhat more realistic current waveform with finite rise and fall times. The design information resulting from this extended analysis provides a more accurate basis for calculation of circuit impedances and operating frequencies while at the same time relaxing the requirement for control of high harmonic terminations.

## II. Rise Time and Harmonic Considerations with Square Wave Current Excitation

Assume the analysis of Ref. 1 (hereafter called the CIN analysis after Clorfeine, Ikola and Napoli) is applied to the diode used for illustration in that reference. The oscillator characteristics are given in Table I. The current and voltage waveforms are shown in Fig. 1. Fourier analysis of the calculated voltage waveforms results in diode impedances at the significant (odd) harmonics as shown in Fig. 2. (The current waveform has no even harmonic content, resulting in infinite impedances at the even harmonic frequencies).

TABLE I

Characteristics of TRAPATT Oscillator Using CIN Analysis (Ref. 1)

| | |
|---|---|
| Diode Type: | Silicon - $p^+nn^+$ |
| n-layer Doping: | $N_d = 10^{15} cm^{-3}$ |
| n-layer Width: | $W = 8 \times 10^{-4} cm$ |
| Saturated Electron Velocity: | $v_{ns} = 1.0 \times 10^7 cm\text{-}sec^{-1}$ |
| Saturated Hole Velocity: | $v_{ps} = 1.0 \times 10^7 cm\text{-}sec^{-1}$ |
| Low Field Electron Mobility: | $\mu_n = 1220\ cm^2\text{-}v^{-1}\text{-}sec^{-1}$ |
| Low Field Hole Mobility: | $\mu_p = 460\ cm^2\text{-}v^{-1}\text{-}sec^{-1}$ |
| Area: | $A = 3.02 \times 10^{-3} cm^2$ |
| Critical Current Density: | $J_c = 1.6 \times 10^3\ A/cm^2$ |
| Peak Current Density: | $J = 3.52 \times 10^3\ A/cm^2$ |
| Normalized Current Density: | $j = J/Jc = 2.2$ |
| Pre-Avalanche Electron Concentration: | $n_o = 10^{10} cm^{-3}$ |
| Multiplication Factor: | $m = 14.5$ |
| Ionization Constant: | $\alpha = 3.69 \times 10^4 cm^{-1}$ |
| Dynamic Breakdown Field: | $E_c = 3.29 \times 10^5\ v\text{-}cm^{-1}$ |
| Period: | $T = 1.06$ nsec |
| Frequency of Operation: | $f = 942$ MHz |

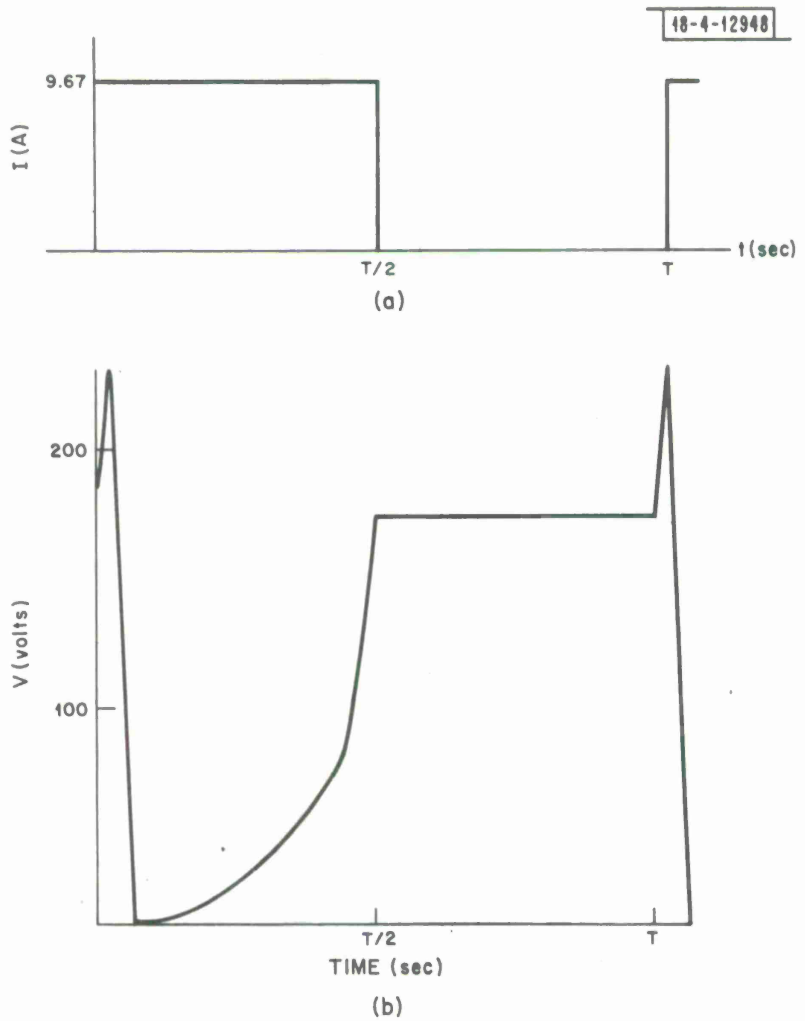


Fig. 1. Waveforms of TRAPATT oscillator using CIN analysis and diode characteristics of Table I. (a) Assumed square wave current drive. (b) Calculated voltage response with linear interpolation in plasma formation interval.

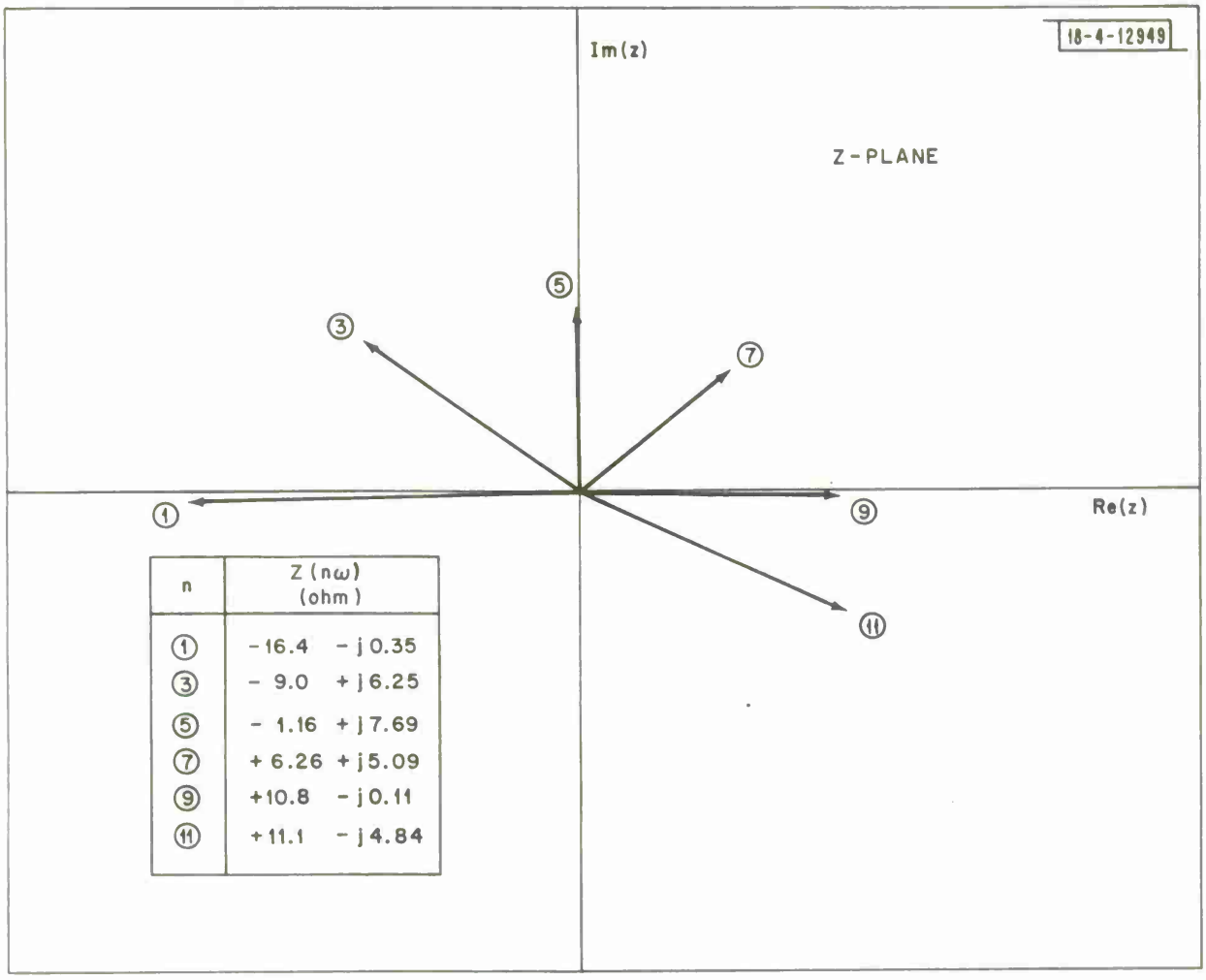


| n | Z (nω) (ohm) |
|---|---|
| ① | -16.4 - j 0.35 |
| ③ | - 9.0 + j 6.25 |
| ⑤ | - 1.16 + j 7.69 |
| ⑦ | + 6.26 + j 5.09 |
| ⑨ | +10.8 - j 0.11 |
| ⑪ | +11.1 - j 4.84 |

Fig. 2. Diode impedances at odd harmonic frequencies for TRAPATT oscillator using CIN analysis and diode characteristics of Table I (junction area A = $3.02 \times 10^{-3} cm^2$).

It is seen in Fig. 2 that the 7th, 9th and 11th harmonics do not represent negative diode resistances. Thus, if the diode is to operate very nearly as analyzed, it is necessary to terminate the high harmonics in negative resistances to provide a match. In other words, the diode must be pumped at these frequencies.

In Ref. 1, this problem is bypassed by neglecting all harmonics above the 5th. It is not always possible to do this. When the high harmonics are eliminated from the square current waveform, the current rise and fall times increase. When this happens, the trapped plasma cycle may be significantly altered. One of the most serious consequences of increasing the current rise and fall times is that premature ionization can occur either because the current does not shut off fast enough at the end of the plasma extraction period or because it does not turn on fast enough at the beginning of the charging period.

Premature ionization must be avoided at the end of the residual extraction period in the high efficiency cycle. If premature breakdown occurs at the end of plasma extraction, the high-voltage low-current portion of the cycle is eliminated and the efficiency of the oscillator is drastically reduced. Premature ionization during the charging period is not as serious a problem, although it may alter the plasma field and plasma carrier concentrations.

The limits on rise and fall time may be examined quantitatively by assuming a drive current with finite rise and fall times. Consider the current fall time first. Assume the current starts to fall at the end of plasma extraction ($t = t_w$). The field $E_w$ at the p - n junction at this time depends on the peak current and the $N_d W$ product. These are chosen so that $E_w < E_b$, where $E_b$ is the static breakdown field. E continues to increase during the current fall time until the current decreases to zero. The final field at the junction is $E_h$, the holding field. If for example, the current is assumed to fall linearly according to the equation

$$J(t) = J - \frac{J}{\tau_f}(t - t_w),\ t_w < t < t_w + \tau_f \tag{1}$$

Then the holding field is given by:

$$E_h = E_w + \frac{1}{\epsilon}\int_0^{t_w + \tau_f} J(t)dt = E_w + \frac{J\tau_f}{2\epsilon} \tag{2}$$

The maximum allowable fall time $\tau_{f\,max}$ to prevent avalanche is obtained by setting $E_h = E_b$, giving:

$$\tau_{f\,max} = (E_b - E_w)\frac{2\epsilon}{J} \tag{3}$$

In reality, the holding field must be less than $E_b$ in order to allow additional time for the current to rise without causing low current ionization at the end of the holding period. The maximum allowable current rise time at the end of the holding period $\tau_{f\,max}$ is calculated in the same way as $\tau_{f\,max}$ assuming the current rises linearly from zero to J in time $\tau_r$.

$$\tau_{r\,max} = (E_b - E_h)\frac{2\epsilon}{J} \tag{4}$$

Equal time intervals may be provided for current turn-on and turn-off by choosing

$$E_h = \frac{E_w + E_b}{2} \tag{5}$$

Then the single critical time constant holds for rise and fall

$$\tau_{max} = (E_b - E_w)\frac{\epsilon}{J} \tag{6}$$

The occurrence of low current ionization during the charge period does not alter the high efficiency cycle in a first order way unless it occurs

before the current has reached the critical level $J_c$ for formation of a traveling ionization zone, where $J_c = qN_d v_{ns}$. If the current reaches the level $J_c$ before the junction field charges to $E_b$, the analysis can be carried out as in the ideal square wave case with appropriate modifications to account for the changing current during the transit of the ionization wave.

A value can be calculated for the maximum allowable transition time $\tau_{max}$ for the sample diode of Table I. For this diode, using $J = 3.52 \times 10^3$ amp/cm$^2$, $E_b = 3.29 \times 10^5$ v/cm, and $E_w = 2.85 \times 10^5$ v/cm:

$$\tau_{max} = 1.3 \times 10^{-11} \text{ sec} \qquad (7)$$

(The value of $E_b$ used here is the dynamic breakdown field $E_c$ of Ref. 1.)

This time may now be compared with the rise time obtained by deleting all the high order Fourier components in the analysis of an ideal square wave with the fundamental frequency given in Table I. Figure 3 illustrates the normalized leading edge waveforms for Fourier synthesized square waves with partial sums varying from 1st harmonic alone to 1st through 11th harmonics. The normalized times required for the various waves to increase from -1 to +1 are tabulated in Table II. Also tabulated are the actual rise times if the period is 1.06 nsec as indicated in Table I.

TABLE II
Rise Times for Waveforms of Fig. 3

| Highest Harmonic Content | Rise Time Normalized to Period | Actual Rise Times for Period T = 1.06 nsec (sec) |
|---|---|---|
| 1 | 0.288 | $3.04 \times 10^{-10}$ |
| 3 | 0.151 | $1.63 \times 10^{-10}$ |
| 5 | 0.101 | $1.07 \times 10^{-10}$ |
| 7 | 0.077 | $8.12 \times 10^{-11}$ |
| 9 | 0.061 | $6.49 \times 10^{-11}$ |
| 11 | 0.051 | $5.42 \times 10^{-11}$ |

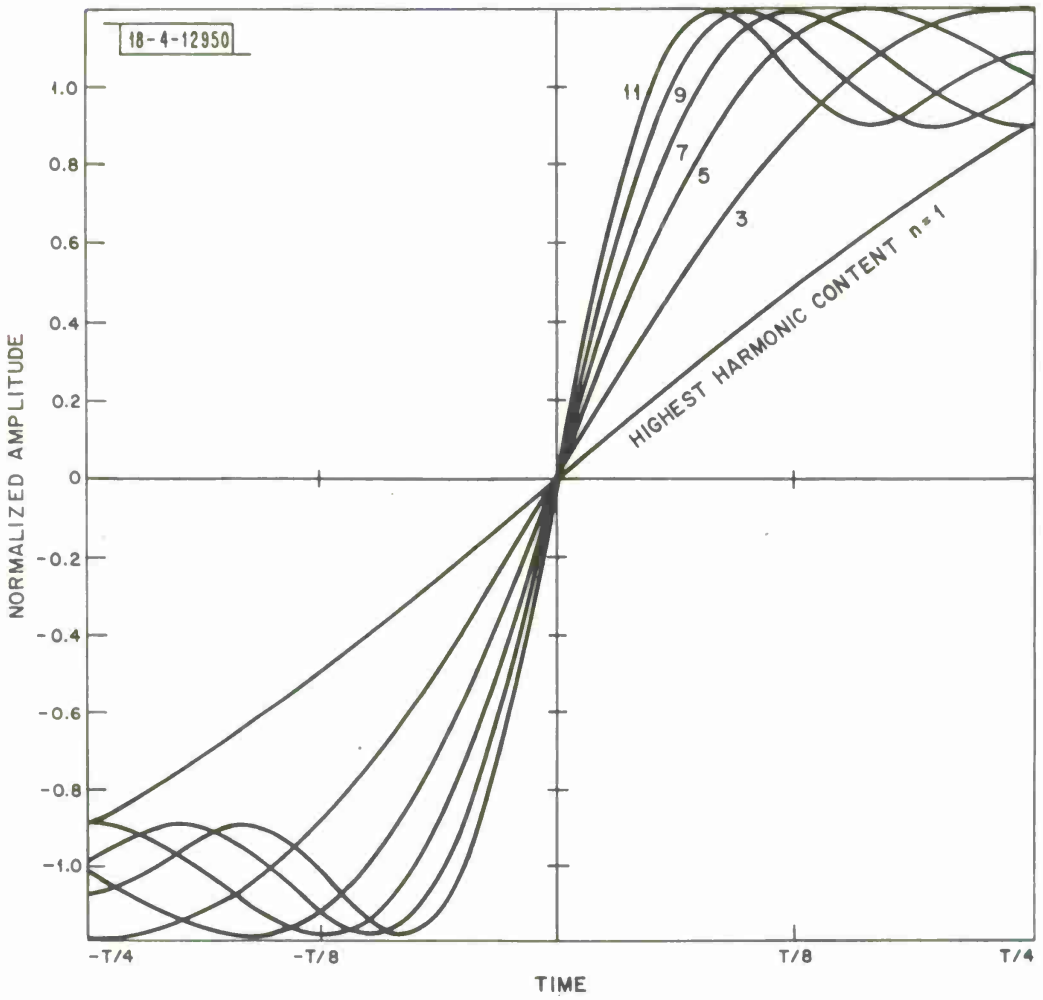


Fig. 3. Leading edge waveforms for partial Fourier sums of an ideal square wave with normalized peak-to-peak amplitude of 2.

A comparison of this tabulation with $\tau_{max}$ indicates that, despite the inclusion of 11 harmonics, the maximum allowable current rise time is exceeded by about a factor of 4.

If only the 5th harmonic is included, $\tau_{max}$ is exceeded by almost a factor of 10. $\tau_{max}$ may be increased without 1st order changes in the high efficiency cycle or analysis. If the $N_d W$ product is decreased, the field at the end of plasma extraction $E_w$ is decreased and, according to Eq. (6), $\tau_{max}$ is increased. Decreasing J also increases $\tau_{max}$. However, when using realistic diode parameters and current densities the square wave analysis does not generally result in $\tau_{max}$ sufficiently large to permit the elimination of harmonics higher than the 5th in the driving waveform. Finite rise and fall times are required for reduced harmonic content in the current waveform. Thus the square wave analysis must be extended to handle plasma formation and plasma extraction under variable current conditions.

## III. Trapezoidal Waveform

It is possible to control the onset of avalanche and simultaneously reduce the harmonic content of the current waveform by increasing the rise and fall times of the current waveform and allowing plasma formation to occur while the current is rising and plasma extraction to continue while the current is falling. For the purpose of analysis, the square wave current is replaced with the ideal trapezoidal waveform of Fig. 4 (solid line). Several trapezoidal waveforms have been investigated. The waveform shown in Fig. 4 has a peak-to-peak rise time which is exactly T/5, where T is the period. This waveform has the special property that its 5th harmonic is identically zero.

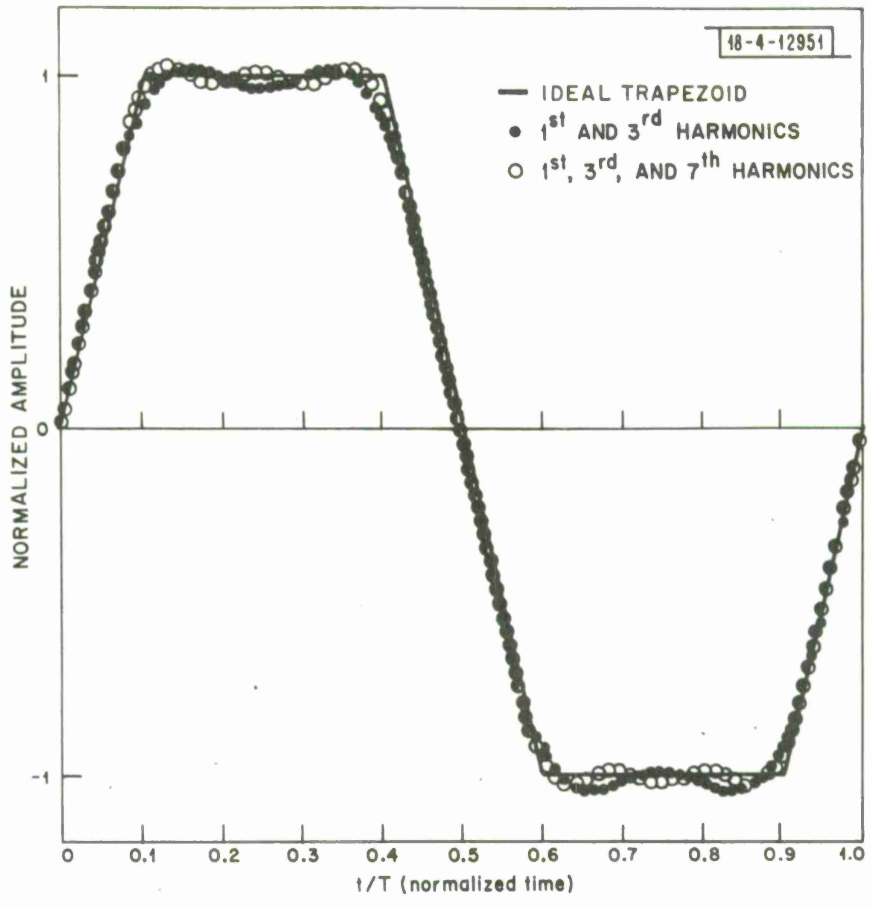


Fig. 4. Trapezoidal driving current waveform with partial Fourier sums.

The amplitudes of the harmonics of this waveform decrease approximately as $1/n^2$. The trapezoidal waveform contains only odd harmonics (a consequence of the fact that $J(t + \frac{T}{2}) = -J(t)$) and when the origin is properly chosen the trapezoidal waveform can be either an even or odd function of time. Fourier analysis of this waveform gives

$$J(t) = \frac{20J_o}{\pi^2}(0.587 \sin\omega t + 0.1056 \sin 3\omega t - 0.0194 \sin 7\omega t - \ldots) \quad (8)$$

It is seen that the amplitude of the 7th harmonic of this waveform is only 3.3% of the fundamental, so that the elimination of harmonics above the third in this waveform has little effect on its shape. This can be seen by examining the dotted and opened curves of Fig. 4 which are plots of partial Fourier sums of this waveform including respectively harmonics through the third and seventh. It is clear that the third harmonic partial sum is a good approximation to the ideal trapezoidal waveform and that the rise time is changed only slightly as the seventh harmonic is added.

## IV. Diode Response to Trapezoidal Current Drive

The solution for the diode's response to this trapezoidal current excitation is based on the same approximations for the ionization coefficient $\alpha$ that were used in Ref. 1. The analysis proceeds along somewhat different lines in that the one cycle of the current waveform is divided into four segments (rise, hold at maximum current, fall, hold at zero current) as opposed to the two segments of the square wave current drive. The resulting voltage waveform still retains the same basic features as that arising from a square wave drive except for a certain amount of smoothing corresponding to the smoothing of the current waveform. The trapezoidal current waveform is divided into ten equal time increments, $\Delta t$. The rise and fall times have a duration of $2\Delta t$ and the flat portion of the waveform has a duration of $3\Delta t$. There is some latitude available in specifying at what point in the current cycle each of the critical transitions in the voltage waveform is

assumed to take place. The operating cycle to be outlined below is one of several that could be chosen. The various transitions in the cycle are chosen either (a) for the sake of analytical convenience, (b) to provide the necessary phase relationship between voltage and current to assure that all significant harmonics can be terminated in positive current, or (c) to assure that the field at the p-n junction remains below the static breakdown field at all times. This analysis has been developed with sufficient generality to allow the rise time of the trapezoidal current waveform and starting time of residual extraction to be varied. These parameters have been selected in the present discussion to provide proper phasing and to prevent premature avalanche with a particular example treated here. Any operating cycle is valid which obeys the diode physics and which leads to self-consistent results and a realizable set of operating impedances. The physical procedure for changing from one realizable operating cycle (or mode) to another is then to alter the current waveform by retuning the external oscillator circuitry and/or by changing the current amplitude.

In the process of searching for realizable current waveforms, it became apparent that the trapped plasma oscillator is not capable of functioning over a wide range of current rise times or amplitudes. The amplitude and rise time must be constrained to lie within relatively narrow values to insure proper phasing to prevent unwanted breakdown transients. This observation is, of course, totally consistent with experimental results. One of the consequences of specifying a ratio of current rise-time to period and a specific time for start of avalanche is that the depletion layer width, doping concentration, and current density can no longer be specified independently. For analytical convenience, the average current density ($J_a$) during plasma formation and the base doping density $N_d$ are chosen as independent variables, and the width and operating frequency become dependent variables. The analysis assumes an ideal $p^+ n n^+$ diode with uniformly doped n region. In the following description the terminology used to describe

the various parts of the cycle will be consistent with that used in Ref. 1. The analysis determines values of electric field and voltage as continuous functions of time during most of this cycle except for plasma formation and residual plasma extraction during which a continuous time dependent voltage waveform is generated by interpolation. In addition, values of base width W and period T are also obtained in the analysis. This description of the analysis will be divided into sections corresponding to the lettered regions shown in Fig. 5. The field profiles corresponding to these regions are plotted in Fig. 6.

A. Charging Period: Region A $(0 \leq t \leq \Delta t)$

The cycle begins at a time when the maximum field in the depletion region is less than the static breakdown field but large enough to cause punch through into the $n^+$ region. At this point the diode voltage is defined as $V_m$ and the peak field is $E_m$, both of which are to be determined. In the absence of ionization there are no free carriers in the depletion region so only displacement current flows:

$$J(t) = \epsilon \frac{\partial E}{\partial t} \tag{9}$$

It can be seen from Fig. 6 that during this interval J(t) is given by

$$J(t) = \frac{J_o}{2\Delta t} t \tag{10}$$

where $J_o$ is the maximum value of the trapezoidal current waveform and is yet to be determined. $\Delta t$ is specified such that the electric field increases from $E_m$ to a value $E_{pk}$ just as the current reaches the level $J_o/2$, giving

$$\Delta t = \frac{4\epsilon}{J_o}(E_{pk} - E_m) \tag{11}$$

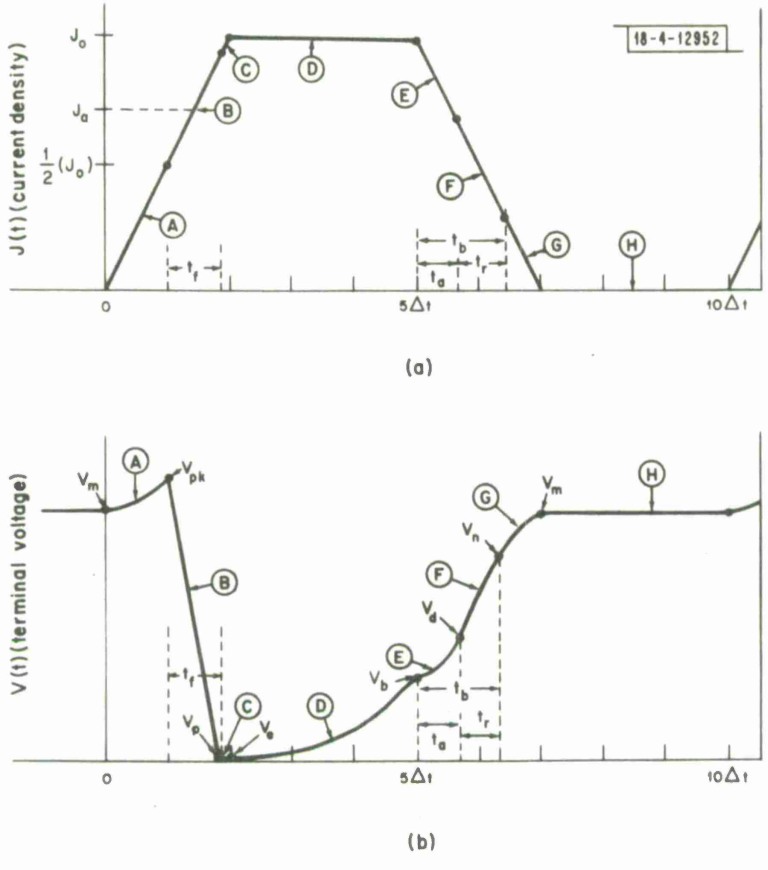


Fig. 5. Waveforms of TRAPATT oscillator using trapezoidal drive. (a) Assumed drive current. (b) Calculated voltage response with linear interpolation in plasma formation interval.

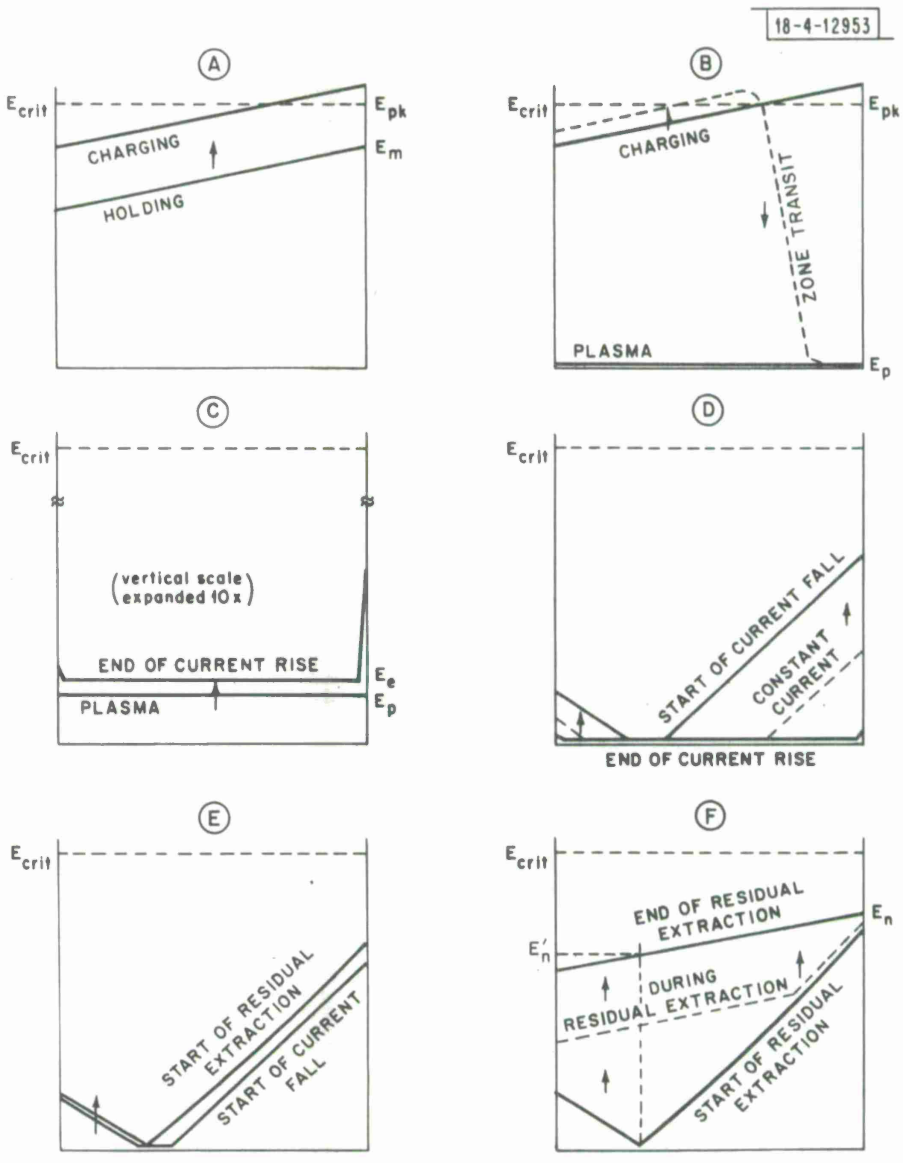


Fig. 6. Approximate field profiles in n-layer of TRAPATT oscillator using trapezoidal current drive. Each diagram illustrates corresponding lettered interval in previous figure.

$E_{pk}$ is the peak field attained at the $p^+n$ junction. Both $E_{pk}$ and $J_o$ can be calculated once $J_a$, the average current density during plasma formation, has been specified. $J_a$ will be discussed in detail in the next section.

The time dependent voltage during this period is:

$$V(t) = V_m + V_{pk}\left(\frac{t}{\Delta t}\right)^2, \quad (0 \leq t \leq \Delta t) \tag{12}$$

where

$$V_{pk} = W\left(E_{pk} - \frac{qN_dW}{2\epsilon}\right). \tag{13}$$

B. Plasma Formation Period: Region B $(\Delta t \leq t < \Delta t + t_f)$

Plasma formation occurs if the current density exceeds a critical value, $J_c = qN_dv_{ns}$ before the junction field has reached its dynamic breakdown level $E_c$. When this happens an ionization zone sweeps across the depletion layer with velocity $v_w$ leaving in its wake a dense plasma of holes and electrons with concentrations $n_p$ and $p_p$. Expressions for the resulting particle concentrations and fields are given in the literature based on the assumption of a constant zone velocity which implies a constant diode current J(t) during the time $t_f$ that the zone is in the depletion layer. In this analysis,the current changes during zone transit. However, it is valid to use the constant current approximation if the zone transit occurs in a time interval which is small compared to the rise-time of the current excitation. The zone transit time is

$$t_f = \frac{W + \delta_s}{J_a} qN_d \tag{14}$$

where $\delta_s$ is the plasma sheath width and $J_a$ is the average current density during zone transit. The quality of the approximation depends on the ratio

$$b_f \equiv \frac{t_f}{\Delta t}. \tag{15}$$

In most cases $b_f$ is approximately 0.5, indicating that the zone transit occupies one-fourth of the rise-time and the approximation is not unreasonable.

In order to make use of the equations for plasma formation previously presented in the literature it is necessary to know the current density during plasma formation. Thus, in this analysis $J_a$ assumes the role of an input parameter in the analysis along with $N_d$. Given $J_a$ and $N_d$ we may proceed directly to calculate all of the plasma parameters. We will follow the analysis presented in Ref. 1 and briefly review here the sequence of expressions derived there for computing the plasma parameters.

First, we define a normalized average current density

$$j_a \equiv \frac{J_a}{qN_d v_{ns}} \tag{16}$$

Then the peak field at the junction is given by

$$E_{pk} = E_c + \frac{qN_d}{\alpha \epsilon}(j_a - 1)\, \ell n\, (\gamma - 1) \tag{17}$$

where

$$\gamma = \left(\frac{j_a + r}{1 + r}\right)\frac{N_d}{n_o} \tag{18}$$

$$\alpha = 2.4 \times 10^{-6} \exp(-1.6 \times 10^{6}/E_{pk})\ \text{cm}^{-1}$$

(the ionization coefficient for silicon)

$$r = v_{ps}/v_{ns} \quad \text{(the ratio of saturated hole and electron velocities)} \tag{19}$$

$$E_c = \left( \frac{\ell n 2}{1.6 \times 10^6} + \frac{1}{E_{pk}} \right)^{-1} \quad \text{(the dynamic breakdown field at the junction)} \tag{20}$$

$$n_o = 10^{10}\,\text{cm}^{-3} \quad \text{(the electron concentration in the depletion layer before ionization)}$$

The plasma field is

$$E_p = \frac{(j_a)^2 v_{ns}}{(j_a + r)(\mu_n + \mu_p)(p_s/N_d) + j_a(\mu_n - \mu_p)} \tag{21}$$

where

$$\mu_n = 1220\ \text{cm}^2\ \text{volt}^{-1}\ \text{sec}^{-1} \quad \text{(the electron mobility)}$$

$$\mu_p = 460\ \text{cm}^2\ \text{volt}^{-1}\ \text{sec}^{-1} \quad \text{(the hole mobility)}$$

$$p_s = \left( \frac{j_a - 1}{j_a + r} \right) n_o e^m \quad \text{(the sheath hole density)} \tag{22}$$

$$m = \ell n\,(\gamma\, \ell n\, \gamma) \quad \text{(the multiplication factor)} \tag{23}$$

The sheath width is

$$\delta_s = \frac{\epsilon E_c}{q(n_s - p_s - n_d)} \tag{24}$$

where

$$n_s = n_o e^m \quad \text{(the sheath electron density)} \tag{25}$$

The plasma electron and hole densities are respectively

$$n_p = \frac{(j_a - 1)v_{ns} n_s}{j_a v_{ns} - \mu_n E_p} \tag{26}$$

$$p_p = \left(\frac{j_a v_{ns} + v_{ps}}{j_a v_{ns} + \mu_p E_p}\right) p_s \tag{27}$$

Although all of the plasma parameters can be calculated at this point, the calculation of depletion layer width W and zone transit time $t_f$, which depends on W must be deferred to a later section.

The time dependence of voltage during plasma formation is relatively complex. We follow the procedure of Ref. 1 and approximate it with a linear decrease in voltage during the zone transit. This approximation is reasonable since the zone transit time $t_f$ is a sufficiently small fraction of the total TRAPATT period that a more detailed analysis would have negligible affect on the efficiency and impedance calculations. Neglecting the effects of the drift of the low velocity electrons during the ionization zone transit and the transient effects as the zone exits the depletion layer a uniform plasma fills the depletion layer after the zone transit is complete. The resulting minimum voltage is then

$$V_p = WE_p \tag{28}$$

Hence the time dependent voltage during zone transit is

$$V(t) = V_{pk} + (V_p - V_{pk})\, t/t_f, \quad (\Delta t \le t \le \Delta t + t_f) \tag{29}$$

C. Rising Current Plasma Region: Region C $\quad (\Delta t + t_f \le t \le 2\Delta t)$

After the plasma has formed, the current density continues increasing until it reaches $J_o$. The current and electric field are ohmically related

in the plasma-filled region so that the electric field also increases linearly during this time. The peak current density $J_o$ can be shown to be related to $J_a$ as

$$J_o = \frac{4J_a}{b_f + 2} \tag{30}$$

and the electric field in the plasma at the end of this period is

$$E_e = \frac{4E_p}{b_f + 2} \tag{31}$$

An exact calculation of the voltage at the end of this period is difficult. However the voltage is negligible compared to the breakdown voltage so that simple approximations may be used with little effect on the final results. Thus, during this interval it is again assumed for purposes of calculating voltage that no plasma drift occurs and the depletion layer remains completely filled with plasma. The resulting end voltage is then

$$V_e = WE_e \tag{32}$$

and the time dependent voltage expression is

$$V(t) = V_p + (V_e - V_p)\left(\frac{t - \Delta t - t_f}{\Delta t - t_f}\right), \quad (\Delta t + t_f \leq t \leq 2\Delta t) \tag{33}$$

In order to determine W it will be necessary to know how far the holes or electrons move during the entire plasma extraction cycle. The distance moved by the holes during this portion of the cycle is

$$d_{p_1} = \int_{\Delta t + t_f}^{2\Delta t} v(t)dt = \int_0^{\Delta t - t_f} \mu_p E'(t)dt \tag{34}$$

where

$$E'(t) = E_p + (E_e - E_p)\frac{t}{\Delta t - t_f} \tag{35}$$

giving

$$d_{p_1} = \frac{\mu_p E_p}{2}\Delta t \frac{(1 - b_f)(6 + b_f)}{2 + b_f} \tag{36}$$

The distance moved by the electrons in the same time is

$$d_{n_1} = \frac{\mu_n}{\mu_p} d_{p_1} \tag{37}$$

D. Constant Current Plasma Region: Region D $(2\Delta t \leq t \leq 5\Delta t)$

As holes drift out of the depletion region they leave behind a region of net negative charge near the $n^+n$ boundary as shown in Fig. 7a. A similar region of net positive charge develops near the $p^+n$ boundary. The departure from neutrality in these two regions results in the approximate field profile shown. We follow Ref. 1 in approximating the field and concentration transitions as abrupt. This is illustrated in Fig. 7b. The velocity in the non-neutral regions is assumed to be saturated. The following expressions for the "residual" particle densities in the saturated velocity regions result from the principle of current continuity:

$$n_r = \frac{(\mu_n + \mu_p)E_e n_p}{v_{ns} + \mu_p E_e} \tag{38}$$

$$p_r = \frac{(\mu_n + \mu_p)E_e p_p}{v_{ps} + \mu_n E_e} \tag{39}$$

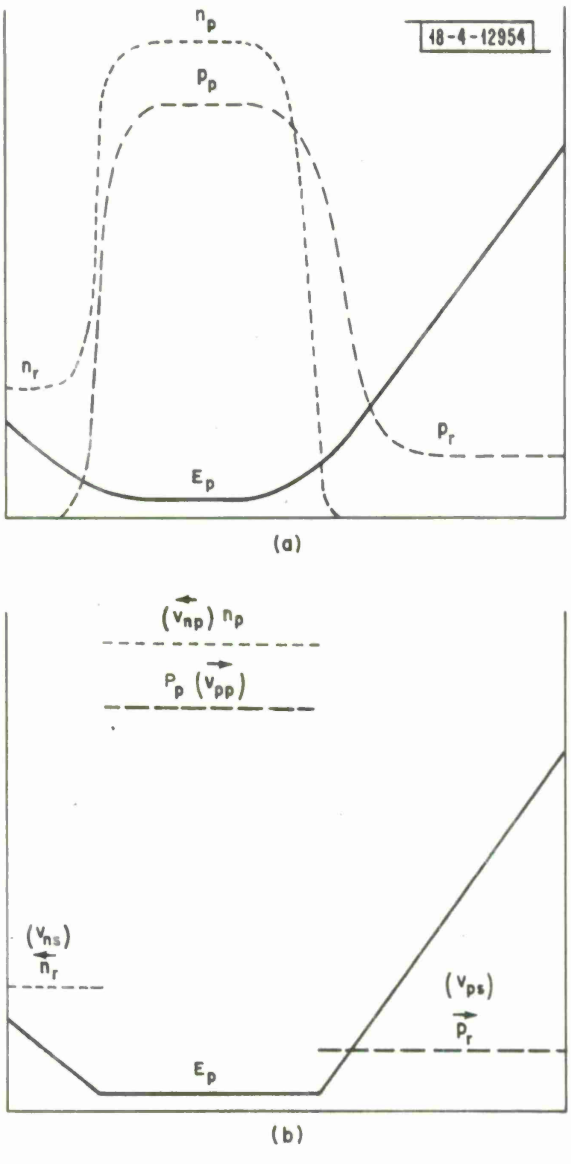


Fig. 7. Electric field and free carrier concentration profiles during plasma extraction period. (a) Actual profiles. (b) Assumed profiles.

To calculate the voltage during this portion of the cycle we must integrate the changing electric field profile of Fig. 7b. The result is the following expression

$$V(t) = E_e W + 1/2 \left\{ S_n \left[ d_{p_1} + d_{p2} \left( \frac{t-2\Delta t}{3\Delta t} \right) \right]^2 + S_p \left[ d_{n_1} + d_{n2} \left( \frac{t-2\Delta t}{3\Delta t} \right) \right]^2 \right\} \tag{40}$$

where

$$S_n = \frac{q}{\epsilon}(n_n - N_d), \; S_p = \frac{q}{\epsilon}(N_d + p_r) \tag{41}$$

are the field gradients in the residual regions, and

$$d_{p2} = 3\mu_p E_e \Delta t, \qquad d_{n2} = 3\mu_n E_e \Delta t \tag{42}$$

are the total distances moved by the trapped carriers during the constant current phase.

E. Falling Current Plasma Region: Region E $(5\Delta t \leq t \leq 5\Delta t + t_a)$

In order to prevent premature avalanche at the end of the plasma extraction process it is necessary to allow the current to begin to fall before the trapped plasma disappears. The beginning of the final saturated velocity plasma recovery phase is assumed to occur $t_a$ seconds after the current starts to fall. For a given set of diode parameters and drive current level there is only a limited range of realizability for $t_a$. If $t_a$ is too short, the n-region is depleted of carriers early, allowing the junction field to charge to breakdown before the current falls to zero. If $t_a$ is long, the free carriers may not be cleared out of the n-layer before current falls to zero. In this analysis it was found that specifying $t_a = 0.4\Delta t$ was sufficient to prevent premature breakdown and to allow time for all the

residual holes and electrons to drift out of the n-layer before the current reaches zero.

The physics of this part of the plasma extraction period is complicated by the falling current. The variation of the carriers and the electric field in this interval are shown in Fig. 8. In this figure the magnitude of the plasma field is expanded out of proportion to the field in the saturated velocity regions. Fig. 8a shows the field and carrier profiles just as the current starts to drop. There is still a fraction of the n-layer filled with the plasma concentration. As the current drops the field in the ohmic plasma region drops also. As a result the residual hole and electron densities in the saturated regions also decrease with time. This is shown in Fig. 8b, where it is clear that the most recently generated residual carriers (nearest the plasma region) have a lower concentration than the older residual carriers. The saturated carrier velocity is about 5 times the plasma velocity so that the reduced carrier concentrations quickly spread out toward the boundaries of the n-layer. In Fig. 8b the holes produced as the current first started to fall have traversed about half the distance to the $p^+n$ junction. As a result of this non-uniform carrier concentration, the electric field profile becomes slightly nonlinear as shown. In Fig. 8c this process has progressed far enough so that the entire region of saturated velocity holes is non-uniformly distributed. Fig. 8d shows the field and carrier profiles at the instant when the trailing edge of the hole packet coincides with the trailing edge of the electron packet and the plasma has just disappeared. This is the beginning of the saturated velocity "residual" extraction period.

We will now proceed to calculate the carrier and field profiles as a function of time during this interval throughout the portion of the n-layer which is filled with residual holes. The electron filled portion may be analyzed in the identical manner with appropriate variable substitutions. The end result is an expression for voltage as a function of time in this interval. During this period the field in the (shrinking) plasma region

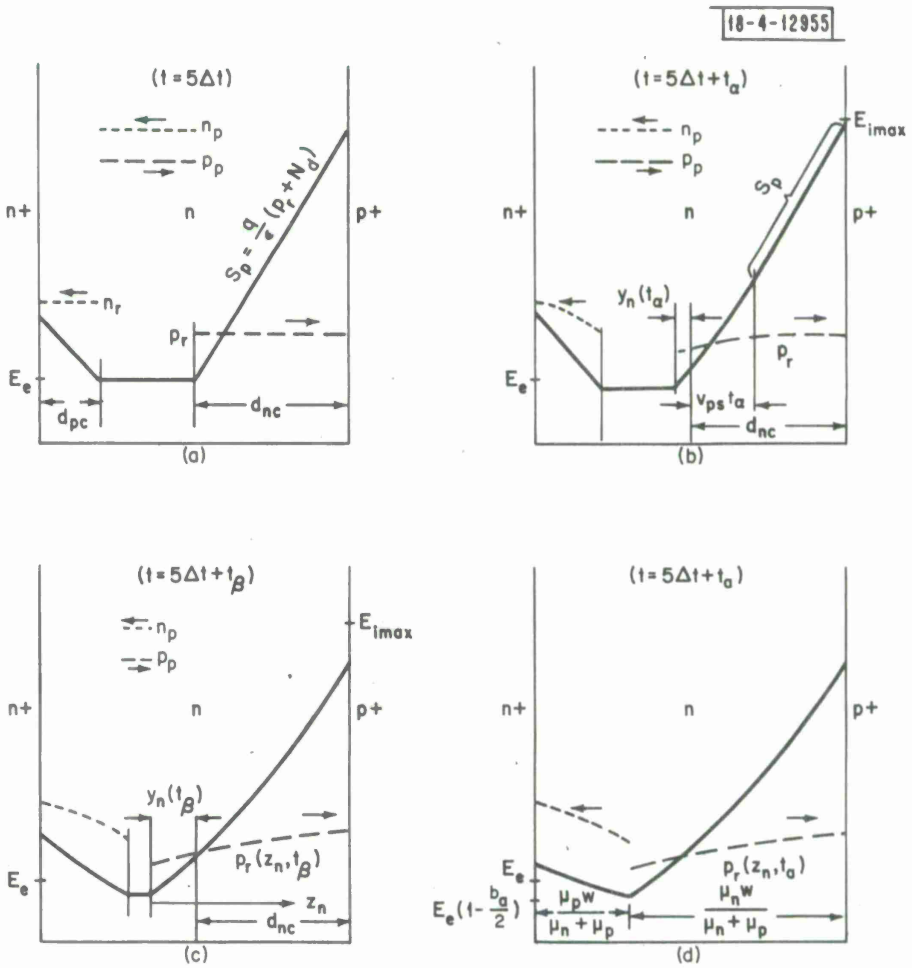


Fig. 8. Field and carrier profiles during falling current portion of plasma recovery cycle from (a) start of current fall to (d) end of plasma extraction.

is given by

$$E_p(t) = E_e\left(1 - \frac{t}{2\Delta t}\right) \tag{43}$$

The distance moved (to the left) by the right hand edge of the plasma region is the distance moved by the trailing edge of the electron packet.

$$y_n = \int_0^{t_y} v_{np}\,dt = \mu_n \int_0^{t_y} E_p(t)\,dt = \mu_n E_e t_y - \frac{\mu_n E_e}{4\Delta t} t_y^2 \tag{44}$$

solving for $t_y = t_y(y_n)$

$$t_y = 2\Delta t \left\{1 + \sqrt{1 - \frac{y_n}{\mu_n E_f \Delta t}}\right\} \tag{45}$$

and substituting into $E_p(t)$ to obtain $E_p(y_n)$

$$E_p(y_n) = E_e \sqrt{1 - \frac{y_n}{\mu_n E_f \Delta t}} \tag{46}$$

This is the field which produces the initial residual hole concentration $p_{r_o}(y_n)$ at the moving right hand edge of the plasma region. $p_{r_o}(y_n)$ is related to $E_p(y_n)$ by

$$p_{r_o}(y_n) = \frac{p_p(\mu_n + \mu_p)E_p(y_n)}{v_{ps} + \mu_n E_p(y_n)} \tag{47}$$

This relation may be linearized by expanding

$$E_p(y_n) = E_e + \Delta E_p(y_n) \tag{48}$$

where $E_e$ is the plasma field at the start of the current fall, and $\Delta E_p(y_n)$ is the change in $E_p(y_n)$. Since $\Delta E_p(y_n) \ll v_{ps}$ we obtain

$$p_{r_o}(y_n) \cong \frac{p_p(\mu_n + \mu_p)}{v_{ps} + \mu_n E_e} E_p(y_n) \equiv C_p E_p(y_n) \tag{49}$$

The residual holes drift to the right with saturated velocity $v_{ps}$. At any time the distribution of holes to the right of the righthand plasma edge is

$$p_r(z_n, t) = C_p E_p\left(y_n(t) - \frac{y_n(t)}{y_n(t) + v_{ps}(t)} z_n\right) \tag{50}$$

where $z_n$ is referenced to a moving coordinate system whose origin is the righthand edge of the plasma zone. $z_n$ increases positively to the right as shown in Fig. 8c. The field in this region of nonuniformly distributed holes may be obtained by integrating Poisson's equation

$$E_p(z_n, t) = \frac{q}{\epsilon} \int_0^{z_n} [N_d + p_r(z'_n)] dz'_n \tag{51}$$

giving

$$E_p(z_n, t) = \frac{q}{\epsilon} \left\{ N_d z_n + C_p E_e \frac{2}{3b} \left[ (a(t) + b(t))^{3/2} - a(t)^{3/2} \right] \right\} \tag{52}$$

where

$$a(t) = 1 - \frac{t}{\Delta t} + \frac{t^2}{4\Delta t^2} \tag{53}$$

and

$$b(t) = \frac{\frac{t}{\Delta t} - \frac{t^2}{4\Delta t^2}}{\mu_n E_f \Delta t \left(\frac{t}{\Delta t} - \frac{t^2}{4\Delta t^2}\right) + v_{ps} t} \tag{54}$$

The voltage drop across the region is then obtained by integrating

$$V_p(t) = \int_0^{d_n} E_p(z_n, t)\, d z_n$$

$$= \frac{q}{\epsilon}\left\{\frac{N_d d_n^2}{2} - C_p E_e \frac{2a(t)}{3b(t)}^{3/2} + C_p E_e \frac{4}{15b^2(t)} \times \right.$$

$$\left. [(a(t) + b(t)d_n)^{5/2} - a(t)^{5/2}]\right\} \qquad (55)$$

where $d_n$, the width of the non-uniform distributed residual hole region, is measured from the edge of the plasma ($z_n = 0$).

If the edge of this region has not drifted to the p-n junction, i.e., $t < d_{nc}/v_{ps}$, (where $d_{nc}$ is the total width of the residual hole saturated velocity region at the start of the current fall), then the voltage in the saturated region includes another term $V_x$ which is the integral of the linear field in the region adjacent to the junction.

$$V_x = E_p(d_n(t), t) \cdot (d_{nc} - v_{ps}t) + 0.5 S_p(d_{nc} - v_{ps}t)^2 \qquad (56)$$

where

$$d_n(t) = y_n(t) + v_{ps}t \qquad (57)$$

Expressions analogous to (55) and (56) can be obtained for the saturated velocity residual electron region. The only remaining component of voltage is then given by the integral of the initial plasma field over the entire n-layer width $W E_e(1 - \frac{t}{2\Delta t})$.

During this time interval it is necessary to keep track of the peak field reached at the junction to assure that premature breakdown does not occur. The rate of change of field at the junction depends both on the external applied current and the drift current of residual holes.

$$\frac{\partial E_j}{\partial t} = \frac{J(t)}{\epsilon} - \frac{q}{\epsilon} p_{rj}(t) v_{ps} \tag{58}$$

where $p_{rj}(t)$ is the instantaneous hole concentration at the junction. From this expression it can be seen that the junction field will reach a maximum and start decreasing when $J(t)$ has decreased sufficiently to make the right-hand side of Eq. (58) equal to zero; i.e., when

$$J_o\left(1 - \frac{t}{2\Delta t}\right) = q\, p_{rj}(t) v_{ps} \tag{59}$$

(assuming this occurs before the residual carriers are completely cleared out of the n-layer).

If this maximum is reached before $p_{rj}(t)$ begins to decrease, the time of occurrence and the magnitude of the maximum junction field are easily calculated.

The time of occurrence measured from start of current fall is

$$t_i = 2\Delta t \left[1 - \frac{J_r}{J_o}\right] \tag{60}$$

where

$$J_r = q\, p_r v_{ps} \tag{61}$$

and $p_r$ is the initial residual hole concentration obtained during the constant current phase.

The maximum field at the junction is

$$E_{imax} = E_{fp} + \frac{J_o \Delta t}{\epsilon} \left(1 - \frac{J_r}{J}\right)^2, \tag{62}$$

where $E_{fp}$ is the junction field at the start of the current fall time. $E_{imax}$ is a relative maximum only, since the field starts rising again when the residual extraction period is complete.

If the maximum field occurs after the residual hole concentration at the junction starts to decrease, the maximum field computation is considerably more complicated. This computation will not be included here because it is not needed in the example to be discussed below.

F. Residual Extraction Region: Region F $(5\Delta t + t_a \leq t \leq 5\Delta t + t_a + t_r)$

When the trailing edges of the unsaturated plasma and hole concentrations coincide as shown in Fig. 8d, the residual plasma extraction period begins. The field now exceeds the saturation level everywhere in the n-layer. In silicon with equal saturation velocities for holes and electrons the remaining time required to completely sweep the depletion region clear of carriers is the time required to remove the residual holes (which have the greater distance to travel.)

$$t_r = \frac{\mu_n W}{(\mu_p + \mu_n) v_{ps}} \tag{63}$$

Exact calculation of a time dependent voltage during this time interval is difficult. For this analysis it suffices to interpolate between the beginning and end voltages.

The field at the end of residual extraction is obtained by starting from the minimum field at the beginning of residual extraction $E_e(1 - \frac{b_a}{2})$ and following it as it charges to a value

$$E_n' = E_e\left(1 - \frac{b_a}{2}\right) + \frac{J_o}{\epsilon}\int_{t_a}^{t_a + t_r}\left(1 - \frac{t}{2\Delta t}\right)dt \tag{64}$$

$$E_n' = E_e\left(1 - \frac{b_a}{2}\right) + \frac{J_o \Delta t}{\epsilon}\left[b_r - \frac{b_a b_r}{2} - \frac{b_r^2}{4}\right] \tag{65}$$

where

$$b_r = \frac{t_r}{\Delta t} \tag{66}$$

at the end of the residual extraction time period.

From Fig. 6f it is seen that the junction field at this time is then

$$E_n = E_n' + \frac{qN_d}{\epsilon}\frac{\mu_n W}{\mu_n + \mu_p} \tag{67}$$

The voltage at the end of residual extraction is simply

$$V_n = E_n W - \frac{qN_d W^2}{2\epsilon} \tag{68}$$

G. Final Charging Region: Region G $(5\Delta t + t_a + t_r \leq t \leq 7\Delta t)$

In this time interval all carriers have been cleared out of the n-layer and the field continues charging under the influence of the decreasing current. We are now able to calculate $E_m$, the junction field at the end of the current fall time, in the same way $E_n$ was calculated, giving

$$E_m = E_e\left(1 - \frac{b_a}{2}\right) + \frac{J_o}{\epsilon}\Delta t\left(1 + \frac{b_a^2}{4} - b_a\right) + \frac{qN_d}{\epsilon}\frac{\mu_n W}{\mu_n + \mu_p}. \tag{69}$$

The time dependent voltage during this period is given most simply as a function of $E_n$

$$V(t) = W\left\{E_n + \frac{J_o}{\epsilon}\left[t - 5\Delta t - \frac{(t - 5\Delta t)^2}{4\Delta t} - \left(t_b - \frac{t_b^2}{4\Delta t}\right)\right]\right\}, \quad (70)$$

$$(5\Delta t + t_b \leq t \leq 7\Delta t),$$

where

$$t_b = t_a + t_r. \quad (71)$$

H. Zero Current Holding Region: Region H $(7\Delta t \leq t \leq 10\Delta t)$

In this time interval the n-layer is depleted of carriers and no current flows. Hence the field profile remains unchanged from its value at the end of interval G. At the end of this interval the TRAPATT cycle is complete.

I. Determination of $t_f$ and W

At this point in the analysis all of the important timing and electric field relations have been derived. However, these expressions depend on the unknown n-layer width W and the avalanche zone transit time $t_f$. Solutions for W and $t_f$ will now be obtained.

The solution for W is based on the fact that the total distance traversed by the trailing edge of the plasma hole packet from the formation of the plasma to the start of residual extraction is

$$d_p = \frac{\mu_p W}{\mu_n + \mu_p}. \quad (72)$$

$d_p$ consists of 3 components as given in Eqs. (36), (42), and (44)

$$d_p = \frac{\mu_p E_p \Delta t\ (1-b_f)(6+b_f)}{2\left(2 + b_f\right)} + 3\mu_p E_e \Delta t + \mu_p E_e \Delta t\ \left[b_a - \frac{b_a^2}{4}\right] \quad (73)$$

Using $E_e = E_p \frac{4}{2+b_f}$, we have

$$W = \Delta t \frac{E_p(\mu_p + \mu_n)}{2(2 + b_f)} (30 + 8b_a - 2b_a^2 - 5b_f - b_f^2). \tag{74}$$

Substituting for $\Delta t$ from Eq. (11) we have

$$W = \frac{a_2}{a_1}(E_{pk} - E_m), \tag{75}$$

where

$$a_2 = \frac{2\epsilon}{J_o} \frac{30 + 8b_a - 2b_a^2 - 5b_f - b_f^2}{2 + b_f} \tag{76}$$

and

$$a_1 = \frac{1}{E_p(\mu_n + \mu_p)} \tag{77}$$

W is an explicit function of $b_f$ and $E_m$ and the dependence of W on $E_m$ can be eliminated as follows: From (69) and using the fact that $E_e << E_m$, $E_m$ may be written as

$$E_m = \frac{J_o}{\epsilon}\Delta t \left(1 + \frac{b_a^2}{4} - b_a\right) + \frac{qN_d}{\epsilon} \frac{\mu_n W}{\mu_n + \mu_p} \tag{78}$$

Using (63)

$$\frac{qN_d}{\epsilon} \frac{\mu_n W}{\mu_n + \mu_p} = \frac{qN_d v_{ps}}{\epsilon} b_r \Delta t \tag{79}$$

$$= \frac{J_o}{\epsilon} \frac{r}{j_o} b_r \Delta t$$

where

$$r = \frac{v_{ps}}{v_{ns}}, \text{ and } j_o = \frac{J_o}{qN_d v_{ns}} \tag{80}$$

So

$$E_m = 4(E_{pk} - E_m)\left[1 + \frac{b_a^2}{4} - b_a + \frac{r}{j} b_r\right] \tag{81}$$

or

$$E_m = E_{pk} \frac{\left(D + \frac{4r}{j_o} b_r\right)}{\left(D + 1 + \frac{4r}{j_o} b_r\right)}, \tag{82}$$

where

$$D = 4 + b_a^2 - 4b_a \tag{83}$$

Substituting (82) into (75) gives

$$W = \frac{a_2}{a_1} E_{pk} \left(1 - \frac{D + \frac{4r}{j_o} b_r}{D + 1 + \frac{4r}{j_o} b_r}\right) \tag{84}$$

$$W = \frac{a_2}{a_1} E_{pk} \left(\frac{1}{D + 1 + \frac{4r}{j_o} b_r}\right) \tag{85}$$

Now return to the solution of $b_f$. By definition

$$b_f = \frac{t_f}{\Delta t} = \frac{W + \delta_s}{\Delta t\, J_a} qN_d = \frac{(W + \delta_s)\, 2qN_d}{\Delta t\, J_o (1 + b_f/2)} \tag{86}$$

$$b_f\,(1 + b_f/2) = \frac{2qN_d}{J_o}\,\frac{W}{\Delta t}\left(1 + \frac{\delta_s}{W}\right)$$

$$= \frac{qN_d}{2\epsilon}\left[\frac{a_2}{a_1} + \frac{\delta_s}{E_{pk}}\,(D + 1 + 4\,\frac{rb_r}{j_o})\right] \tag{87}$$

Now

$$b_r = \frac{\mu_n E_p}{v_{ps}}\,\frac{J_o a_2}{4\epsilon} \tag{88}$$

So

$$b_f\left(1 + \frac{b_f}{2}\right) = \frac{qN_d}{2\epsilon}\,\frac{(D + 1)\delta_s}{E_{pk}} + \left\{\left[E_p(\mu_n + \mu_p) + \frac{\delta_s \mu_n E_p qN_d}{E_{pk}\,\epsilon}\right] \times \right.$$

$$\left. \frac{qN_d}{J_o}\left(\frac{2C - 5b_f - b_f^{\,2}}{2 + b_f}\right)\right\} \tag{89}$$

where

$$C \equiv 15 + 4b_a - b_a^{\,2}. \tag{90}$$

Using Eq. (30) we have

$$b_f(1 + \frac{b_f}{2}) = k_1 + k_2\,\frac{(1 + b_f/2)\,(2C - 5b_f - b_f^{\,2})}{2 + b_f}\,, \tag{91}$$

where

$$k_1 = \frac{qN_d}{2\epsilon}\,\frac{(D + 1)\,\delta_s}{E_{pk}} \tag{92}$$

$$k_2 = \left[ E_p(\mu_n + \mu_p) + \frac{\delta_s \mu_n E_p q N_d}{E_{pk} \epsilon} \right] \frac{q N_d}{2 J_a} . \qquad (93)$$

The result is a cubic equation in $b_f$ which can be easily solved for its real, positive root:

$$b_f^3(1 + k_2) + b_f^2(4 + 7k_2) + b_f(4 - 2k_1 - [2C - 10]k_2)$$

$$-(4k_1 + 4Ck_2) = 0 \qquad (94)$$

This completes the TRAPATT analysis.

J. Numerical Results

This section gives the results of a sample calculation using the analysis described above. The diode parameters are assumed identical to those listed in Table I with the following exceptions:

a. The normalized average current density during the avalanche is $j_a = 2.2$.

b. The n-layer width W is not specified as an input parameter.

c. The peak current $J_o$ is not specified as an input parameter.

d. The normalized time from the start of the current fall to the start of residual extraction is $b_a = 0.4$.

The results of the calculation are given in Table III. The computed voltage waveform for one cycle is given in Fig. 9.

It is seen that the junction field does not exceed the static breakdown value of $3 \times 10^6$ v/cm except during avalanche formation. The n-layer width is 7.496$\mu$m, the frequency is 1.49 GHz, and the peak current density is $5.33 \times 10^3$ A/cm$^2$. These results may be compared with the results obtained by applying the C.I.N. square wave analysis to a diode of the same width and assuming the same peak current. The outcome of that calculation is summarized in Table IV. The resulting frequency is 948 MHz. Because of the large peak current density of $5.33 \times 10^3$ A/cm$^2$, premature avalanche occurs in this diode during plasma extraction despite the assumption of an ideal square wave current drive.

Harmonic impedances are obtained by Fourier analyzing the voltage waveform of Fig. 9. Table V gives the calculated impedances through the 7th assuming a junction area of $10^{-3}$ cm$^2$. The efficiency and average voltage are also given. In the 2nd column of Table V these values are compared with the corresponding results obtained by analysis of the voltage waveform for the square wave case of Table IV. It is seen that the 7th harmonic impedance is positive in the square wave case. This means that an active termination would be required for an exact match at this frequency. However, as we have seen in Fig. 4, the elimination of the 7th harmonic current in the trape-

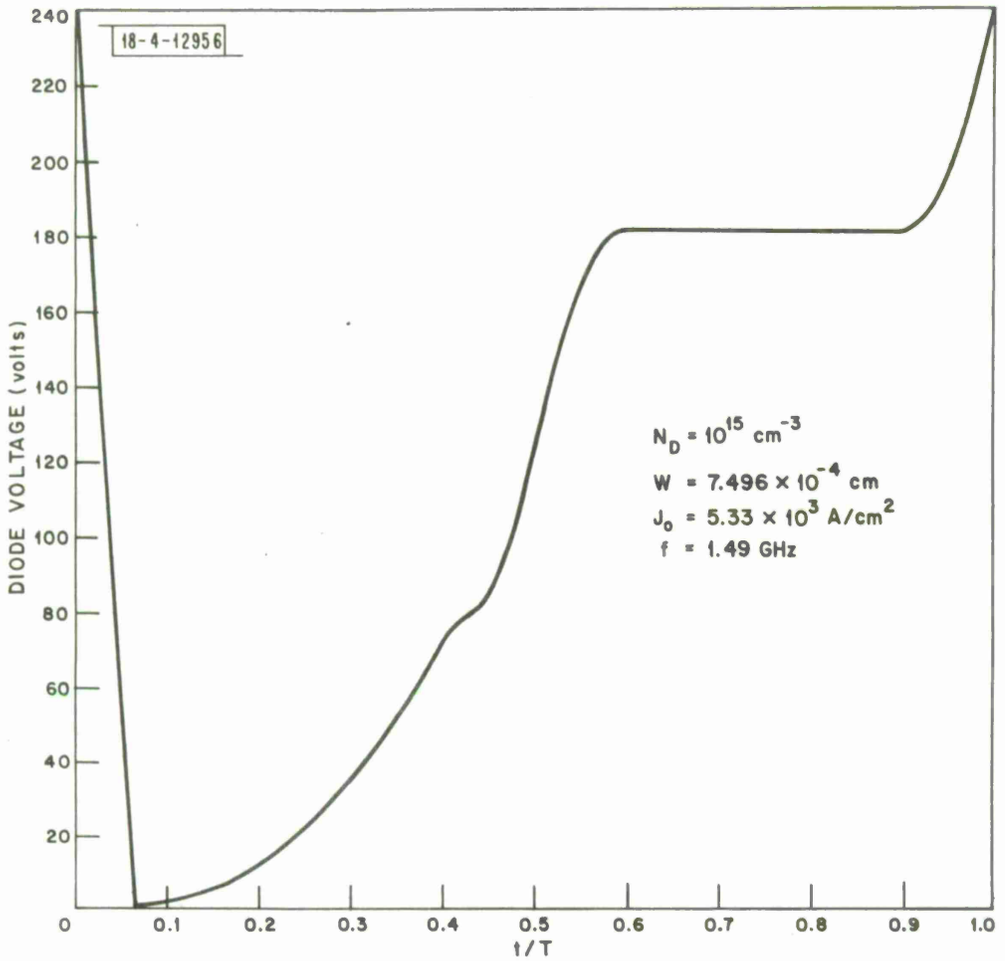


Fig. 9. One cycle of voltage waveform computed for TRAPATT oscillator, driven by trapezoidal current. Diode and operating parameters for this case are given in Table III. Current rise time is 0.2T.

TABLE III

Summary of Trapezoidal Current Calculation for TRAPATT Oscillator

Diode Parameters

Same as in TABLE I except N-Layer Width (W): Not Specified

Input Parameters

Normalized Current Density During Avalanche ($j_a$): 2.2
Normalized Time to Residual Extraction ($b_a$): 0.4
Peak Current Density ($J_o$): Not Specified

Junction Field Calculations

Start of Plasma Formation ($E_c$): $3.29 \times 10^5$ v/cm
Maximum During Plasma Formation ($E_{pk}$): $3.83 \times 10^5$ v/cm
End of Plasma Formation ($E_p$): $1.20 \times 10^3$ v/cm
End of Current Rise ($E_e$): $1.82 \times 10^3$ v/cm
Start of Current Fall ($E_{fp}$): $2.65 \times 10^5$ v/cm
Maximum During Residual Extraction ($E_{max}$): $2.83 \times 10^5$ v/cm
End of Residual Extraction ($E_n$): $2.47 \times 10^5$ v/cm
Holding Field ($E_m$): $2.99 \times 10^5$ v/cm

Other Results

N-Layer Width (W): $7.496 \times 10^{-4}$ cm
Peak Current Density ($J_o$): $5.33 \times 10^3$ A/cm$^2$
Normalized Time for Plasma Formation ($b_f$): 0.642
Frequency (f): 1.49 GHz
Average Voltage: 115.6v
Efficiency: 48.8%

TABLE IV

Summary of Square Wave Current Calculations for TRAPATT Oscillator of Table III

Diode Parameters

Same as Table I except: $W = 7.496 \times 10^{-4}$ cm

Input Parameters

$J_o = 5.33 \times 10^3$ A/cm2

$j_a = 3.331$

Junction Field Calculations

$E_c = 3.63 \times 10^5$ v/cm

$E_{pk} = 4.31 \times 10^5$ v/cm

$E_p = 1.04 \times 10^3$ v/cm

Frequency

f = 0.948 GHz

Average Voltage

129.0v

Efficiency

52.9%

TABLE V

Impedances of TRAPATT Oscillators of Tables III and IV

Assuming Junction Area of $10^{-3}$ $cm^2$

| Harmonic Number | Impedance (Ohms) (Trapezoidal) | Impedance (Ohms) (Square Wave) |
|---|---|---|
| 1 | -30.1 + j 0.286 | -33.6 - j 2.98 |
| 3 | -37.4 + j 32.8 | -21.7 + j 8.9 |
| 5 | 0.0 | -12.0 + j 14.4 |
| 7 | + 20.4 - j 94.0 | -6.7 + j 16.32 |

zoidal waveform has little effect on the shape or rise time of the waveform. Thus, the 7th harmonic may be terminated in an open circuit without affecting the trapezoidal analysis in a first-order way, leaving a requirement for complex impedance terminations only at the fundamental and third harmonics. All other harmonics, both even and odd are terminated in open circuits. From Table V it is seen that the fundamental impedances in both cases are approximately pure real and differ in magnitude by only about 10%. In the trapezoidal case the real part of the 3rd harmonic impedance is nearly double the corresponding impedance in the square-wave case. The reactive component is more than a factor of three larger. The larger 3rd harmonic impedance results principally because the 3rd harmonic of the trapezoidal current waveform is twice that of the square wave.

The magnitude of the 3rd harmonic impedance is also higher than the magnitude of the fundamental impedance in the trapezoidal case, making it easier to realize the 3rd harmonic termination experimentally.

The efficiency in the square-wave case is 52.9% as compared to 48.8% in the trapezoidal case. This approximate 6% difference in efficiency occurs primarily because the ratio of fundamental to dc in the trapezoidal current waveform is approximately 6% less than the same ratio for the square cur-

rent waveform, while the resulting ratios of fundamental to dc voltage are identical to within 1% in the two analyses.

## K. Conclusions

An approximate analysis of TRAPATT operation has been described which employs physically realizable waveforms and which results in realistic conditions on the oscillator harmonic terminations. This analysis is based on specific assumptions concerning the shape of the driving current waveform and the timing of the critical transitions in the diode. It is thus more of an existence demonstration than a general analysis of TRAPATT operation.

The results demonstrate the realizability of continuous high efficiency oscillations in an idealized avalanche diode structure using a trapezoidal current waveform. The calculations also indicate that while a previous TRAPATT analysis assuming an ideal square wave current gives a reasonable approximation to the fundamental impedance and efficiency, the 3rd and 5th harmonic impedances are significantly altered in going from the unrealizable square wave to the realizable trapezoidal current drive.

One of the principal reasons for developing a finite rise time analysis was to better understand and prevent premature avalanche at the end of the plasma extraction period. The results of this trapezoidal analysis indicate that premature avalanche can be avoided when using a finite fall time current drive if the current fall begins early in the plasma extraction process. However, it is clear that precise waveform control is required to accomplish this, and that small variations in operating frequency or harmonic terminations could result in major changes in the operating mode of the oscillator. Thus, an oscillator operating in this finite rise-time or trapezoidal current mode will be inherently narrowband and will operate only over a small range of 3rd and 5th (in this case the 5th is an open circuit) harmonic impedances.

## REFERENCES


1. A. S. Clorfeine, R. J. Ikola, and L. S. Napoli, "A Theory for the High-Efficiency Mode of Oscillation in Avalanche Diodes," RCA Review, Vol. 30, No. 3, pp. 397-421,(Sept. 1969).

2. B. C. Deloach, Jr. and D. L. Sharfetter, "Device Physics of TRAPATT Oscillators," IEEE Trans. Electron Devices, Vol. ED-17, No. 1 pp. 9-21, (Jan. 1970).

3. D. L. Scharfetter, "Power Frequency Characteristics of the TRAPATT Diode Model of High-Efficiency Power Generation in Germanium and Silicon Avalanche Diodes," B. S. T. J., Vol. 49, No. 5, pp. 799-826, (May-June 1970).

## DOCUMENT CONTROL DATA – R&D

*(Security classification of title, body of abstract and indexing annotation must be entered when the overall report is classified)*

| | |
|---|---|
| 1. ORIGINATING ACTIVITY *(Corporate author)*<br>Lincoln Laboratory, M.I.T. | 2a. REPORT SECURITY CLASSIFICATION<br>Unclassified<br>2b. GROUP<br>None |

3. REPORT TITLE

An Analysis of Finite Rise and Fall Time Current Excitation of TRAPATT Diodes

4. DESCRIPTIVE NOTES *(Type of report and inclusive dates)*

Technical Note

5. AUTHOR(S) *(Last name, first name, initial)*

Bryant, Thomas G. and Welch, Jerry D.

| | | |
|---|---|---|
| 6. REPORT DATE<br>7 January 1971 | 7a. TOTAL NO. OF PAGES<br>48 | 7b. NO. OF REFS<br>3 |
| 8a. CONTRACT OR GRANT NO. F19628-70-C-0230<br>b. PROJECT NO. 649L<br>c.<br>d. | 9a. ORIGINATOR'S REPORT NUMBER(S)<br>Technical Note 1971-2<br>9b. OTHER REPORT NO(S) *(Any other numbers that may be assigned this report)*<br>ESD-TR-71-3 | |

10. AVAILABILITY/LIMITATION NOTICES

This document has been approved for public release and sale; its distribution is unlimited.

| | |
|---|---|
| 11. SUPPLEMENTARY NOTES<br>None | 12. SPONSORING MILITARY ACTIVITY<br>Air Force Systems Command, USAF |

13. ABSTRACT

Several recent papers have treated the high efficiency avalanche diode using a simplified analysis which successfully explains the principal features of the traveling avalanche zone, formation of the trapped plasma, and plasma extraction. These analyses have assumed square wave current excitation so that all phenomena occur under constant current conditions. In this paper it is shown that the square wave current excitation requires negative impedance terminations above the 5th harmonic. Since the harmonic amplitudes in a square wave decrease only as 1/n, harmonics as high as the 9th and 11th must be properly terminated to make the analysis realistic and to prevent premature avalanche. We have analyzed the TRAPATT operation using the same physical approximations for plasma formation and recovery as used in the previous square wave analyses. However, we have assumed a trapezoidal current waveform which contains primarily first and third harmonics with negligibly small higher harmonics. In this analysis the avalanche zone transit and portions of the plasma extraction process occur while the current is changing. The resulting device voltage is calculated as a continuous analytical function of time except during the plasma formation interval and the final saturated velocity phase of the plasma extraction interval, where an interpolated voltage waveform is obtained. Fourier analysis of the voltage waveform provides the device efficiency as well as the necessary circuit termination at the 1st and 3rd harmonics. Realizability conditions on the diode parameters are also obtained.

14. KEY WORDS

TRAPATT diodes avalanche diodes waveforms